Bull. Mater. Sci. (2021) 44:249
https://doi.org/10.1007/s12034-021-02542-y

Boltzmann equation for the modelling of formation of silver nanoparticles using trisodium citrate as the reducing agent

JADHAV PANKAJ NAGNATH, DELPHY DAVIS, P OVIA, SAMDAVID SWAMINATHAN and KANNAN DEEPA*

Department of Chemical Engineering, SRM Institute of Science and Technology, Kattankulathur 603203, India
*Author for correspondence (kdeepa86@gmail.com)

MS received 19 January 2021; accepted 8 July 2021

Abstract. The kinetics of formation of silver nanoparticles using trisodium citrate as the reducing agent was studied in order to evaluate the rate constants and the rate expression. The inability to measure the concentration of the reactant (precursor silver salt) at millimolar concentrations using conventional spectrophotometric techniques renders the studies of kinetics cumbersome. An attempt was made to study the kinetics of this reaction by measuring the concentration of silver nanoparticles instead of the silver ions as a function of time. The initial concentration of the reducing agent (trisodium citrate) was taken to be nearly 20 times that of the initial concentration of the silver ions. Hence, the reaction could be modelled as pseudo-first-order kinetics, considering the bimolecular nature of the reaction. The final second-order rate constant was evaluated using integral method of analysis as 0.254 l (g min)$^{-1}$. The key steps in the formation of silver nanoparticles (i.e., reduction, nucleation, growth and saturation) were modelled as a sigmoidal plot using Boltzmann equation. A very good fit of experimental data ($R^2 \approx 0.99$) was observed with the model.

Keywords. Silver nanoparticles; chemical kinetics; modelling; Boltzmann equation.

1. Introduction

Metal nanoparticles possess interesting optical and electronic properties, which are highly dependent on their shape and size. Among the metal nanoparticles, silver has gained significant attention from both the research and industrial community alike, one of the reasons being their cost-effective synthesis by chemical means. The anti-bacterial effects and nonlinear optical properties of silver nanoparticles render them useful in several applications [1,2]. A variety of nanosilver-based products have been commercialized, thereby increasing the demand to synthesize nanoparticles in large scale. The medical and environmental applications of silver nanoparticles are abundant owing to their anti-oxidant, anti-microbial and anti-neoplastic properties [3,4]. Recently, nanostructures have also been used in plasmon-enhanced solar water splitting for the generation of hydrogen [5]. Nanocomposites of silver in combination with metal oxides have potential photocatalytic applications [6]. The design of suitable reactors to cater to the escalating nanotechnology market requires the knowledge of chemical reaction kinetics. Metal nanoparticles can be synthesized by physical approaches, such as laser ablation and evaporation, while chemical approaches involve the bottom-up building up of metal atoms into clusters and then nanoparticles. Chemical reduction methods offer additional advantages such as the control of size and shape of the nanoparticles by controlling reaction conditions [7].

Among the wet chemical synthesis methods, sodium borohydride- or trisodium citrate-mediated reduction of silver ions are desirable in terms of reproducibility and economic viability [8]. The study of kinetics of chemical reactions becomes tedious when the concentration of the reactant or the product is difficult to determine by simple analytical methods, such as UV–visible spectrophotometry. Since Ag^+ ions did not exhibit a characteristic absorption peak in the UV–visible spectra, the reaction kinetics can be studied by estimating the concentration of silver nanoparticles. An attempt was made in this direction to study the kinetics of formation of silver nanoparticles using trisodium citrate as the reducing agent. Subsequently, a model predicting the sigmoidal behaviour of the stages involved in the formation of silver nanoparticles has been proposed.

2. Experimental

2.1 *Materials*

Silver nitrate (extra pure, 99.5%) was procured from Sisco Research Laboratories Private Ltd, Mumbai, Maharashtra, India. This was used as the precursor salt for synthesizing

Published online: 08 September 2021

silver nanoparticles. The solution of silver nitrate was freshly prepared every time before use. Trisodium citrate dihydrate (extra pure, 99%) was procured from Merck Specialities Private Ltd, Worli, Mumbai, Maharashtra, India. This was used as the reducing agent. The chemicals were used as received without further purification. Distilled water was used for all the experiments and analyses.

2.2 *Synthesis of Ag nanoparticles*

A 500 ml of 0.0169 g l^{-1} silver nitrate solution $\left(C_{0,Ag^+} = 0.01 \text{ g } l^{-1}\right)$ was prepared in distilled water. The solution was taken in a three-neck round-bottomed flask fitted with a reflux condenser and kept in an oil bath, and heated using an electric heating mantle. A 10 ml of 10 g l^{-1} aqueous solution of trisodium citrate was prepared. When the temperature of the silver nitrate solution turns 100°C, the trisodium citrate solution was added. The concentration of trisodium citrate in the reaction mixture at the start of the reaction $\left(C_{0,Na_3citrate}\right)$ is 0.196 g l^{-1}. The reaction mixture was continuously stirred at 450 rpm throughout the process.

2.3 *Characterization*

The absorption values and spectra were recorded using a Cary 60 UV-visible spectrophotometer from Agilent Technologies. The morphology of the silver nanoparticles was captured using a JEOL Japan, JEM-2100 Plus high-resolution transmission electron microscope (HRTEM). The concentration of silver was measured using a Perkin Elmer Optima 5300 DV inductively coupled plasma–optical emission spectrometer (ICP-OES). When the reaction is complete, the contents of the round-bottomed flask were cooled to room temperature and then centrifuged at 12,500 rpm at 0°C for 30 min. After centrifugation, the silver nanoparticles settled down while the unreacted Ag^+ ions remained in the supernatant. The settled pellet was further washed in distilled water three to four times before sample characterization using ICP-OES. The total silver content in the supernatant was also analysed.

2.4 *Kinetics and modelling*

To obtain kinetic data, samples were collected after the addition of trisodium citrate at regular intervals of 5 min up to 100 min or later, i.e., until no further change in absorbance was observed. Any further reaction was arrested in the collected samples by 'freeze quenching' before characterization. An attempt was also made to model the formation of silver nanoparticles using Origin Pro 8 software.

3. Results and discussion

3.1 *Synthesis and characterization of silver nanoparticles*

On adding the trisodium citrate solution to a boiling solution of silver nitrate, the solution gradually turned straw yellow and then yellowish brown. The UV–visible spectra of the samples collected at intervals of 5 min from the start of the reaction showed a distinct surface plasmon resonance (SPR) peak of silver nanoparticles around 430 nm. The broad absorption band from 200 to 300 nm corresponds to Ag^+ ions [9]. The initial nucleation step was observed for the first 20 min of the reaction, resulting in the formation of Ag^0 nuclei. The subsequent growth phase ($\sim$21 to 60 min) involved the secondary deposition of Ag^0 atoms on the pre-formed nuclei. The third phase (beyond 60 min) is the saturation phase, where electrostatic stabilization of the nanoparticles is facilitated by the excess reducing agent itself. After around 70 min, there were no changes in the intensity of the SPR peak (figure 1a). In order to confirm the presence of silver nanoparticles, samples were drop coated onto carbon-coated copper grids and analysed using HRTEM. Triangular (edge length $\sim$70 nm) and rod-shaped (35 to >100 nm in length) particles were obtained in addition to a few irregular shapes (figure 1b).

3.2 *Kinetics of formation of nanoparticles*

The kinetic experiments were carried out by isolation method, i.e., taking one of the reactants in excess. The initial concentration of trisodium citrate $\left(C_{0,Na_3citrate} = 0.196 \text{ g } l^{-1}\right)$ was twenty times that of the initial concentration of Ag^+ ions $\left(C_{0,Ag^+} = 0.01 \text{g } l^{-1}\right)$. Hence, the reaction leading to the formation of silver nanoparticles can be studied as pseudo-first order [10].

$$-\frac{dC_{Ag^+}}{dt} = k.C_{Ag^+}.C_{Na_3citrate} \quad (1)$$

$$-\frac{dC_{Ag^+}}{dt} = k'.C_{Ag^+} \quad (2)$$

where

$$k' = k \cdot C_{Na_3citrate} \quad (3)$$

Here, C_{Ag^+} is the concentration of silver ions at any time 't', $C_{Na_3citrate}$ is the concentration of trisodium citrate at any time 't', k is the second-order rate constant, and k' is the pseudo-first-order rate constant. Since the absorption spectra of Ag^+ ions did not give a sharp peak, the kinetic studies were carried out by measuring the concentration of Ag nanoparticles. The chemical reaction leading to the formation of silver nanoparticles from silver nitrate using trisodium citrate as the reducing agent has been reported [11].

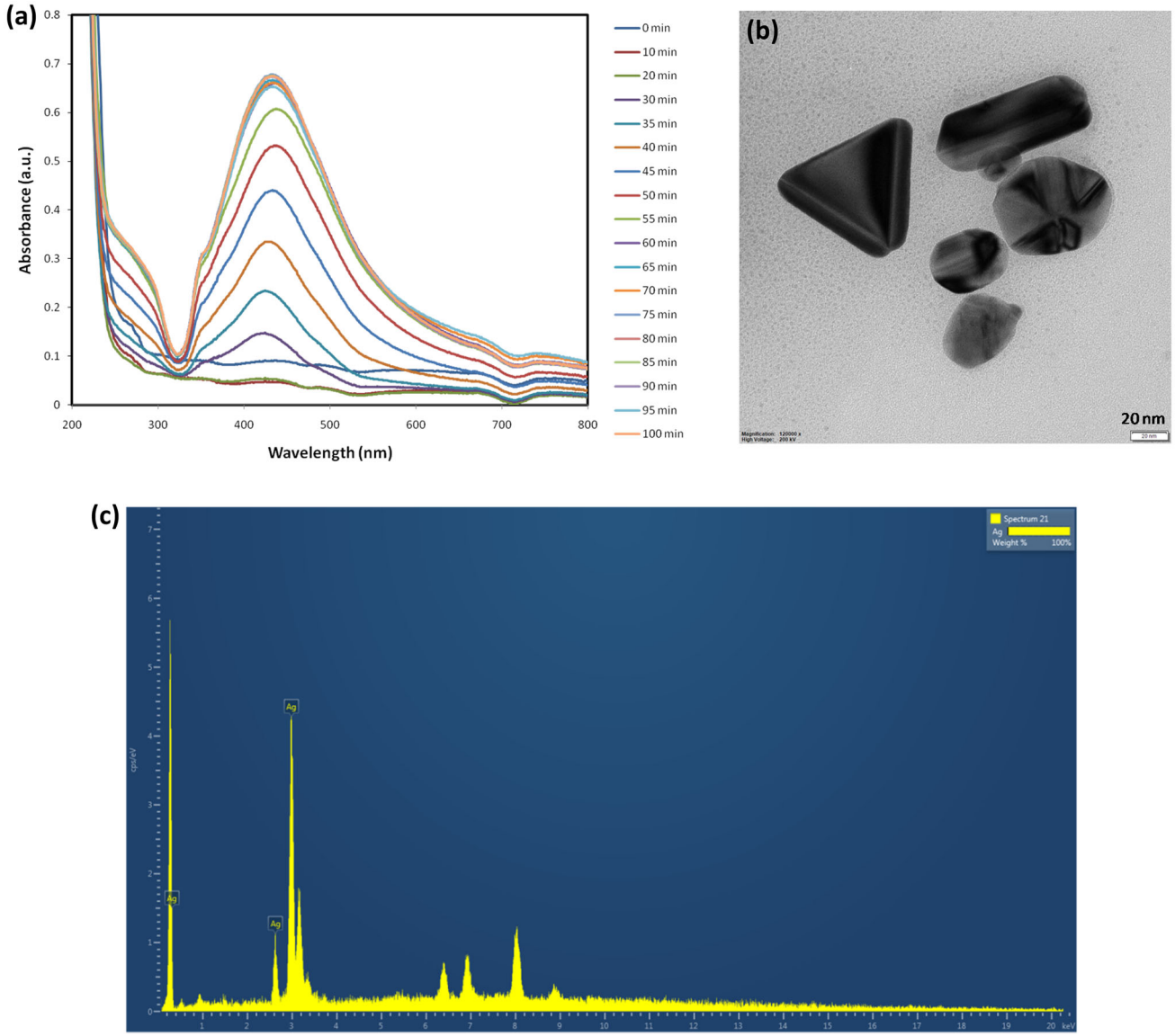

Figure 1. (**a**) UV–visible absorption spectra of silver nanoparticles during the reaction, showing the evolution of SPR band with time (conditions: $C_{0,Ag^+} = 0.01\text{g l}^{-1}$, $C_{0,Na_3citrate} = 0.196\text{g l}^{-1}$, temperature = 100 ± 1°C), (**b**) HRTEM image of silver nanoparticles synthesized by reduction using trisodium citrate and (**c**) EDX spectrum of the silver nanoparticles.

$$4\ Ag^+ + C_6H_5O_7Na_3 + 2\ H_2O \rightarrow 4\ Ag^0 + C_6H_5O_7H_3 + 3\ Na^+ + H^+ + O_2 \uparrow \quad (4)$$

Since the silver ions are converted into silver nanoparticles alone, the fraction of the Ag^+ ions reacted represents the concentration of silver nanoparticles produced.

$$X_A = \frac{C_{0,Ag^+} - C_{Ag^+}}{C_{0,Ag^+}} = \frac{C_{0,Ag^+}.X_A}{C_{0,Ag^+}} = \frac{C_{Ag}}{C_{0,Ag^+}}, \quad (5)$$

where X_A is the fractional conversion of Ag^+ ions to Ag nanoparticles, C_{0,Ag^+} is the initial concentration of Ag^+ ions (g l^{-1}), C_{Ag^+} is the final concentration of Ag^+ ions at any time (g l^{-1}), and C_{Ag} is the concentration of silver nanoparticles at any time (g l^{-1}). The concentration of silver ions in the supernatant obtained after centrifugation of the colloidal silver nanoparticles was determined by ICP-OES as 0.274×10^{-3} g l^{-1}. This value is the final concentration of Ag^+ ions after the completion of the reaction. Since the initial concentration of Ag^+ ions, C_{0,Ag^+} was 0.01 g l^{-1}, the fractional conversion of silver ions to silver nanoparticles, X_A was found to be 0.97. The concentration of the silver nanoparticles was calculated from equation (5) for different dilutions of the colloidal silver nanoparticles. The calibration plot of absorbance at 430 nm *vs.* the concentration of silver nanoparticles of different dilutions was used for further calculations of concentration from absorbance data.

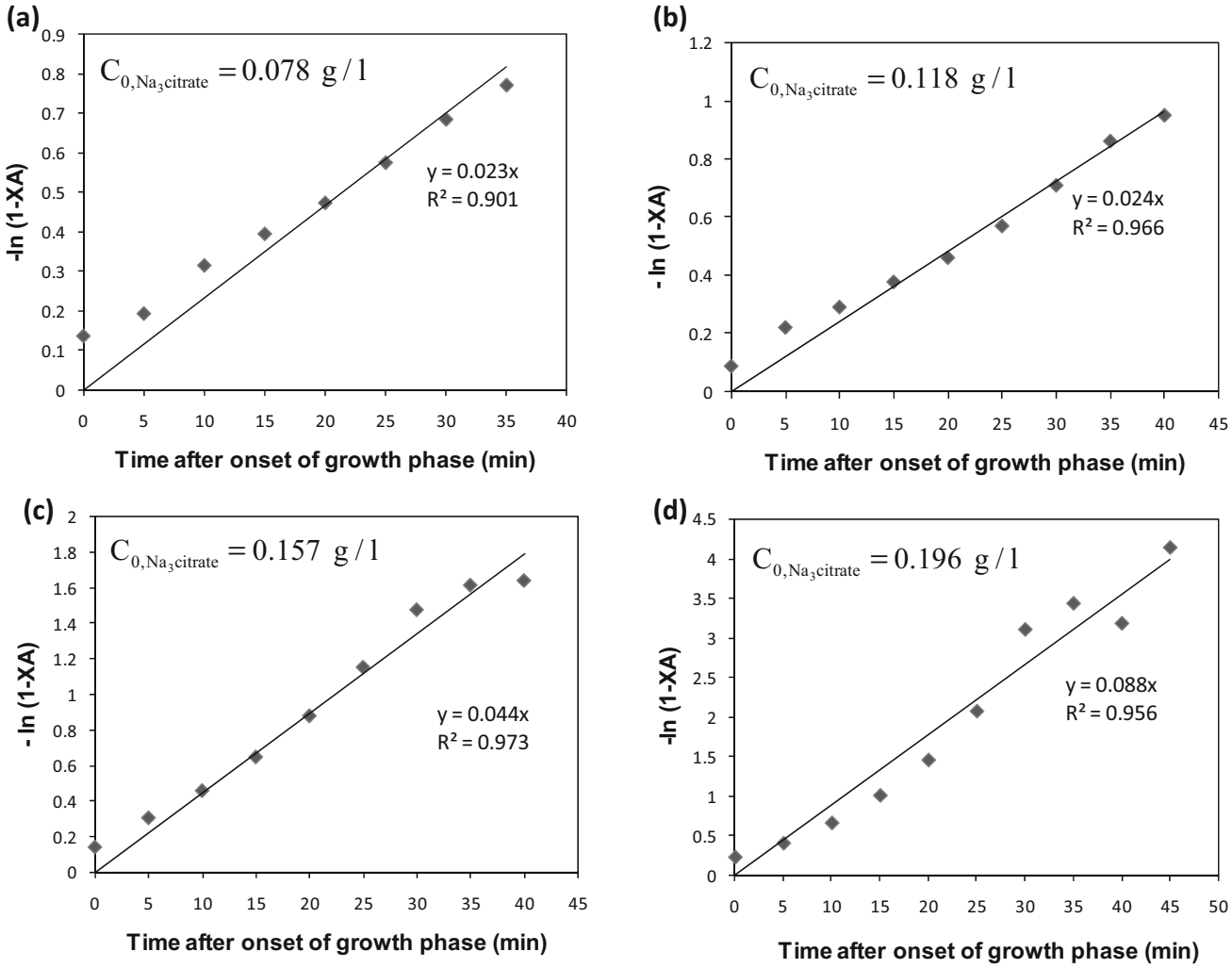

Figure 2. Determination of first-order rate constants for different initial concentrations of trisodium citrate. The initial concentrations of trisodium citrate are (**a**) 0.078, (**b**) 0.118, (**c**) 0.157 and (**d**) 0.196 g l^{-1}.

The pseudo-first-order rate constant, k' was estimated by plotting a graph of $-\ln(1 - X_A)$ *vs.* time for different initial concentration of trisodium citrate, $C_{Na_3citrate}$ (figure 2). The role of citrate on the kinetics was studied by varying the initial concentrations of trisodium citrate as 0.078, 0.118, 0.157 and 0.196 g l^{-1}.

Since the concentration of silver nanoparticles increases in a sigmoidal fashion, linearity of the data was observed only in the growth phase. Hence the time period of growth phase was taken as the Y-axis. The slopes of these plots gives the k' values [12]. The change in concentration of trisodium citrate did not affect the sigmoidal trend of formation of silver nanoparticles. However, the plot of $-\ln(1 - X_A)$ *vs.* time was used to determine the apparent rate constant, k', which was used in calculating the actual second-order rate constant.

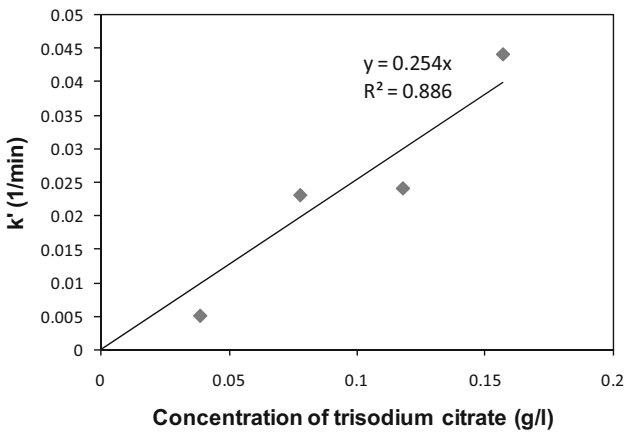

Figure 3. Determination of second-order rate constant for the reaction leading to the formation of silver nanoparticles.

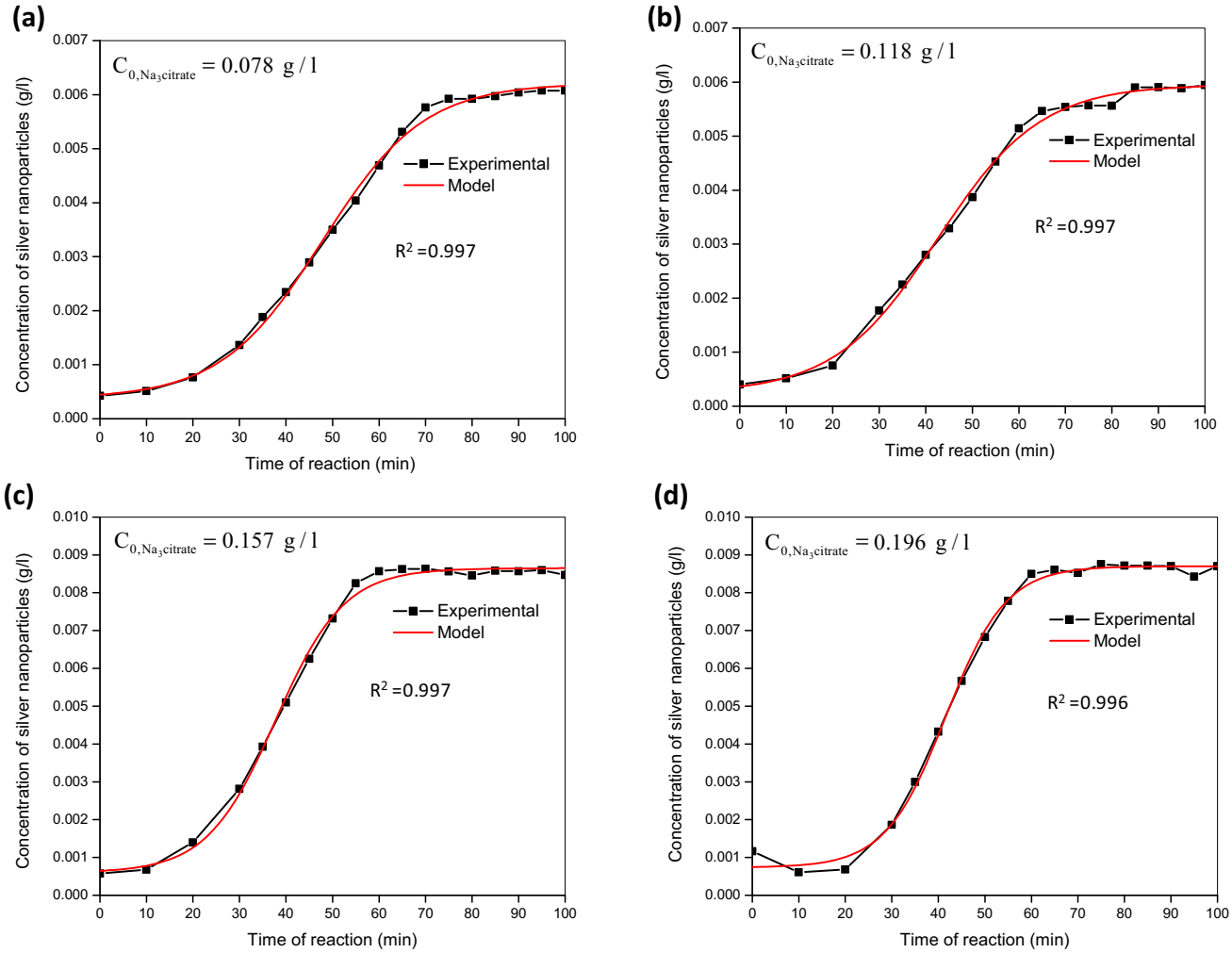

Figure 4. Modelling the formation of silver nanoparticles using Boltzmann equation. The initial concentrations of trisodium citrate used in the study are (**a**) 0.078, (**b**) 0.118, (**c**) 0.157 and (**d**) 0.196 g l^{-1}.

Table 1. Comparison of experimental data and model for the formation of silver nanoparticles.

Concentration of trisodium citrate (g l^{-1})	Parameters				Regression coefficient, R^2
	$C_{Ag,min}$(g l^{-1})	$C_{Ag,max}$(g l^{-1})	t_0 (min)	dt (min)	
0.078	$3.74 \times 10^{-4} \pm 8.9 \times 10^{-5}$	$0.0062 \pm 6.5 \times 10^{-5}$	47.825 ± 0.59	10.904 ± 0.57	0.9974
0.118	$2.42 \times 10^{-4} \pm 1.1 \times 10^{-4}$	$0.0059 \pm 6.4 \times 10^{-5}$	42.530 ± 0.706	11.07 ± 0.67	0.9965
0.157	$5.96 \times 10^{-4} \pm 1.3 \times 10^{-4}$	$0.0086 \pm 6.4 \times 10^{-5}$	37.730 ± 0.47	7.360 ± 0.42	0.9969
0.196	$7.3 \times 10^{-4} \pm 1.2 \times 10^{-4}$	$0.0087 \pm 7.3 \times 10^{-5}$	41.569 ± 0.47	6.483 ± 0.41	0.9962

In order to determine the actual second-order rate constant, the k' values were plotted against different concentrations of trisodium citrate (figure 3). The slope of this linear plot gives the second-order rate constant, k as 0.254 l (g min)$^{-1}$.

3.3 *Modelling the formation of nanoparticles*

The sigmoidal trend of formation of silver nanoparticles was modelled using Boltzmann equation in OriginPro8. The experimental data and the model were in very good

agreement as seen from the R^2 values (figure 4). The parameters and R^2 values are given in table 1. The Boltzmann equation perfectly fits the pattern of formation of silver nanoparticles and is given by equation (6).

$$C_{\mathrm{Ag}} = C_{\mathrm{Ag,max}} + \frac{\left(C_{\mathrm{Ag,min}} - C_{\mathrm{Ag,max}}\right)}{1 + \exp\left(\frac{t - t_0}{\mathrm{d}t}\right)}, \tag{6}$$

where C_{Ag} is the concentration of silver nanoparticles at any time (g l^{-1}), $C_{\mathrm{Ag,min}}$ and $C_{\mathrm{Ag,max}}$ are the minimum and maximum concentrations of the silver nanoparticles (g l^{-1}), t is the time of reaction (min), t_0 is the time (min) at which the concentration of silver nanoparticles is exactly half way between $C_{\mathrm{Ag,min}}$ and $C_{\mathrm{Ag,max}}$, and dt is the slope of the curve. Unlike other previously reported models, the Boltzmann equation reported herein perfectly fits the experimental data of concentration of silver nanoparticles *vs.* time of reaction encompassing all the different stages of formation of the nanoparticles (figure 4). The nucleation phase, growth phase and saturation phase are clearly discernible in figure 4a–d. Previously, Šileikaitė *et al* [13] have modelled the formation of silver nanoparticles by fitting an exponential function to the experimental data of SPR peak position *vs.* boiling time.

4. Conclusions

The kinetics of formation of silver nanoparticles using trisodium citrate as the reducing agent was investigated and the rate constant of the second-order reaction was found to be 0.254 l (g min)$^{-1}$. The stages involved in the formation of silver nanoparticles could be predicted using Boltzmann equation with an excellent fit. The parameters of the equation were also deduced at different concentrations of trisodium citrate. This study is perhaps the first of its kind to model the formation of nanoparticles using the Boltzmann equation commonly used in electrochemistry.

Acknowledgements

We acknowledge the HRTEM facility at SRMIST, set up with support from MNRE (Project No. 31/03/2014-15/PVSE-R&D), Government of India, for the electron micrographs. We also thank the Sophisticated Analytical Instrument Facility (SAIF), IIT Madras, for the ICP-OES analysis.

References

[1] Sondi I, Goia D V and Matijević E 2003 *J. Colloid Interface Sci.* **260** 75
[2] Rai M, Yadav A and Gade A 2009 *Biotechnol. Adv.* **27** 76
[3] Lara H H, Ixtepan-Turrent L, Jose Yacaman M and Lopez-Ribot J 2020 *ACS Appl. Mater. Interfaces* **12** 21183
[4] Sivakumar M, Surendar S, Jayakumar M, Seedevi P, Sivasankar P, Ravikumar M *et al* 2020 *J. Cluster Sci.* **1** 1
[5] Atabaev T S 2018 *Mater. Sci.* **12** 207
[6] Sanzone G, Zimbone M, Cacciato G, Ruffino F, Carles R, Privitera V *et al* 2018 *Superlattices Microstruct.* **123** 394
[7] Rafiquee M Z A, Siddiqui M R, Ali M S, Al-Lohedan H A and Al-Othman Z A 2015 *Bioprocess. Biosyst. Eng.* **38** 711
[8] Deshpande J B and Kulkarni A A 2018 *Chem. Eng. Technol.* **41** 157
[9] Htwe Y Z N, Chow W S, Suda Y and Mariatti M 2019 *Mater. Today* **17** 568
[10] Luty-Blocho M, Pacławski K, Jaworski W, Streszewski B, Fitzner K 2011 in V Starov and K Procházka (eds) *Trends in colloid and interface science XXIV* (Berlin, Heidelberg: Springer) p 39
[11] Rashid M U, Bhuiyan M K H and Quayum M E 2013 Dhaka Univ. *J. Pharm. Sci.* **12** 29
[12] Levenspiel O 1998 *Chemical reaction engineering* (New York: John Wiley & Sons) p 44
[13] Šileikaitė A, Puišo J, Prosyčevas I and Tamulevičius S 2009 *Mater. Sci. (Medžiagotyra)* **15** 21